Nat Hazards (2012) 62:657–676
DOI 10.1007/s11069-012-0100-1

ORIGINAL PAPER

Mapping the susceptibility to sinkholes in coastal areas, based on stratigraphy, geomorphology and geophysics

S. Margiotta · S. Negri · M. Parise · R. Valloni

Received: 29 September 2011 / Accepted: 21 January 2012 / Published online: 3 February 2012

Abstract Sinkholes and land subsidence are among the main coastal geologic hazards. Their occurrence poses a serious threat to the man-made environment, due to the increasing density of population, pipelines and other infrastructures along the coasts, and to the catastrophic nature of the phenomena, which generally occur without any premonitory signs. To assess the potential danger from sinkholes along the coast, it is important to identify and monitor the main factors contributing to the process. This article reports a methodology based on sequential stratigraphic, hydrogeological and geophysical investigations to draw up a susceptibility map of sinkholes in coastal areas. The town of Casalabate situated in the Apulia region (southern Italy), affected by a long history of sinkhole phenomena, is here presented as an example. The approach proposed is based on sequential stratigraphical, geomorphological and geophysical surveys to identify the mechanisms of sinkhole formation and to provide a zonation of the areas in which further sinkhole phenomena may likely occur. Interpretation of the ground penetration radar and electrical tomography profiles has enabled us to identify the potentially most unstable sectors, significantly improving the assessment of the sinkhole susceptibility in the area. The proposed methodology is suitable to be exported in other coastal areas where limestone bedrock is not directly exposed at the surface, but covered by a variable thickness of recent deposits.

Keywords Sinkhole · Karst · Coastal areas · Geophysics · Apulia

S. Margiotta · S. Negri
Hydrogeophysics and Stratigraphic Laboratory for Environmental Risk,
Department of Material Science, University of Salento, Lecce, Italy

M. Parise (✉)
National Research Council of Italy, IRPI, Bari, Italy
e-mail: m.parise@ba.irpi.cnr.it

R. Valloni
Department of Earth Sciences, University of Parma, Parma, Italy

1 Introduction

The carbonate bedrock of coastal areas may be affected by ground instability, which frequency and distribution depends upon a number of factors including, but not limited to, morphology (beaches vs. cliffs), lithology (hard calcarenites, sands, limestones, etc.), development of natural karst caves, presence of anthropogenic cavities, etc.

Development of sinkholes may be particularly severe in coastal karst areas (Forth et al. 1999), where both natural and anthropogenic processes contribute to accelerate the dissolution of carbonate rocks and subsidence processes, and influence the coastline evolution. Among the several cases described worldwide, Norris and Back (1990) report the geomorphic consequences of the groundwater mixing zones along the coast of Yucatan in Mexico. There, the formation of lagoons occurs through several phases: development of subsurface dissolution conduits evolving into cave systems strongly guided by fracture patterns; collapse of the cave roofs; formation of lagoons; erosion by biological activity; degradation through erosion by wave action.

The shape of the coastline may be therefore heavily controlled by subsidence and/or sinkhole phenomena, which development and evolution may result in the formation of bays, inlets and represent the main factor in the overall configuration of the coast. This is especially true for low-lying coasts in soluble deposits, which is the case for most of the Apulian coastlines of southern Italy, on both the eastern (Adriatic) and western (Ionian) sides (Fig. 1).

In this region, previous studies have described the presence of extensive systems of sinkholes along the Ionian coastline at Torre Castiglione (Bruno et al. 2008), where their evolution appeared to be influenced by tectonics, with elongated strips of structurally controlled sinkhole features, in a setting where development of caves is favored by mixing between fresh and brackish water. Farther south, the Palude del Capitano area shows a more advanced stage of evolution, with wide basins connected by submerged passages, only a part of which has been so far explored by divers (Denitto et al. 2006).

Fig. 1 Study area, and location of the sites mentioned in the text. *Gray spots* indicate the distribution of Holocene coastal marsh deposits

A similar situation can be recognized on the opposite side of Apulia, facing the Adriatic Sea (Fig. 1): the Cesine area hosts a some 3 km^2 swamp environment over a local bedrock of Early Pleistocene calcarenites. Delle Rose and Parise (2002) reconstructed the evolution of this area starting from the development of individual sinkholes, their later widening through failures from the margins, the coalescence among adjacent features, up to the present situation, with more than one-third of the overall area occupied by water. Farther south, the coastline is characterized by higher rock cliffs with sinkholes generally occurring as collapse individual phenomena, only locally coupled or multiple (Delle Rose and Parise 2004, 2005).

Whether the coastline characters and the sinkhole typologies, sinkholes represent, combined with coastal erosion, the main geohazard in Apulia (Delle Rose et al. 2004; Parise 2008; Del Prete et al. 2010), and should deserve careful attention by land planners and administrators in order to reduce the related risk. To provide a contribution in this direction, we present in this paper a multi-disciplinary approach addressed to the identification of sinkhole-prone areas in low-lying sectors of the Apulia coasts. The site of Casalabate has been selected for the study, due to high frequency of occurrence of sinkholes in the last decades (Fig. 2), combined with a heavy human pressure during the summer season, which makes the area highly vulnerable and with several significant elements at risk.

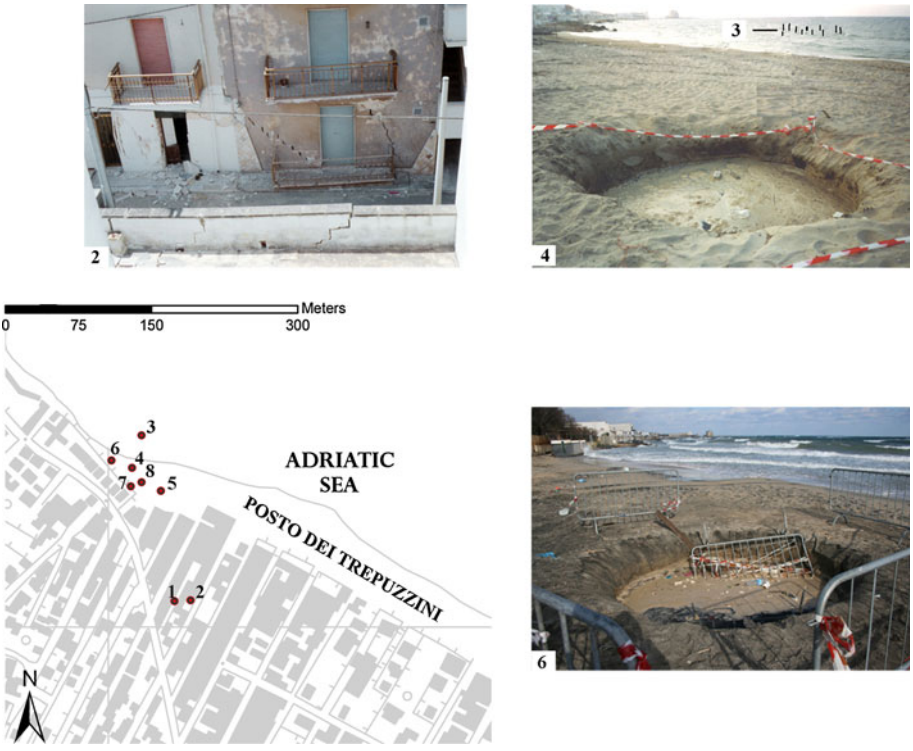

Fig. 2 Location of sinkhole events at Casalabate (numbering as in Table 1). *Inset photos 2*, *4* and *6* illustrate some of the sinkhole events, and their effects

2 Geological and geomorphological setting

The Salento peninsula (southern portion of Apulia region) is a typical Mediterranean area, which is bounded to the east by the Adriatic sea, to the west by the Ionian sea and to the north by the Murge plateau (Fig. 1). From Brindisi to Taranto, the Salento shorelines include more than 400 km of rocky coasts, cliffs and beaches. Rocky coasts are widespread from Otranto to Taranto where mostly thin Middle-Upper Pleistocene marine terraced deposits (Cotecchia et al. 1971; Hearty and Dai Pra 1992) characterize 130 km of the shoreline. Terraced deposits are very often associated with eolian dune deposits which form dune belts sub-parallel to the relict coastlines (Cotecchia et al. 1969; Palmentola 1987; Mastronuzzi and Sansò 2002; De Waele et al. 2011a). These deposits, also termed eolianites because of their carbonate composition, are generally well cemented bioclastic calcarenites with high angle cross-lamination and deformational structures interpreted as seismites (Moretti 2000), or as deformation in soft sediments induced by ancient sinkhole activity (Moretti et al. 2011). Back dune deposits characterized by massive red continental clayey sands are also locally associated. On the Adriatic side, from Otranto to Capo Santa Maria di Leuca, cliffs formed by several carbonate systems of Cretaceous, Eocene and Oligocene age (Bosellini et al. 1999) crop out spectacularly for about 15 km.

Beaches dominate a great part of Ionian (for about 60 km) and Adriatic (50 km extended from Brindisi to Otranto) shorelines. Further 30 km consist of beaches bordered landward by active retreating cliffs. Holocene beach deposits with dune belt and back dune deposits cover a Miocene, Pliocene and Lower Pleistocene carbonate bedrock (Bossio et al. 2006; Margiotta et al. 2010). The Holocene eolian dune deposits, cropping out mainly along the present shoreline, are assigned to three different units of mid-Holocene, Greek-Roman and Medieval age (Mastronuzzi and Sansò 2002). During the Holocene, because of the sea level rise, a number of lacustrine basins, marshes and lagoons were present along the Salento coastlines (Margiotta 1997; Harding 1999; Boenzi et al. 2006; Primavera et al. 2011).

From the hydrogeological standpoint, the aquifer hosted in Cretaceous to Oligocene limestone formations is the major local fresh water source. Multi-layered shallow aquifers in Miocene, Pliocene and Pleistocene rocks have limited extension and variable thickness, thus being less exploited than the main aquifer (Margiotta and Negri 2005).

3 Study area

The study area of Casalabate is located in north-eastern Salento. It was chosen as test site because of the geological, geomorphological and hydrogeological complexity, the occurrence of numerous sinkhole phenomena in recent years and the presence of a human community, which strongly increases during the summer season (over 40,000 people).

With respect to the Casalabate historical coastal tower the shoreline is characterized by a low rocky coast (maximum height 1 m) to the north and by a sandy beach, bordered by a discontinuous belt of dunes to the south. These coastal dunes are backed by wide ponds and coastal swamps (Posto dei Trepuzzini) that were reclaimed in the 1950–1960 period. Further inland, partially covered by topsoil and/or recent continental deposits, a series of Pleistocene deposits are recognized. The town of Casalabate extends close to the shoreline so that in many cases the town expansion resulted in destruction of the dune belt. From 1993 to 2011, several sinkholes occurred (Table 1; Fig. 2) causing irreparable damage and destruction of buildings, and sinking of a portion of the emerged and submerged beach.

Table 1 Characteristics of the eight sinkhole events registered at Casalabate in the past 18 years (1993–2011)

No	Date	Shape	Width (cm)	Depth (cm)	Damage	Type	Notes
1	January 6, 1993	n.d.	n.d.	n.d.	Roads	cs	Sinking of ~40 cm
2	January 1, 1994	n.d.	n.d.	n.d.	Buildings	cs	Same area as in no. 1, sinking ~130 cm
3	August 20, 1997	Circular	~100	200	Bathing prohibition	cc	Shoreface, fresh water spring
4	May 15–19, 2000	Circular	>300	~70		cc (?)	Beach, some 30 m from no. 3
5	November 17, 2004	Circular	~80	40–50		cc	~30 south of no. 4, onshore
6	March 2, 2010	Circular	300	200	Buildings at risk	cc	
7	November 6, 2010	Circular to triangular	10–25	10 (max)		cs	Small-size features (excluding two of greater dimensions)
8	March 10, 2011	Circular	100	45		cc (?)	

Key to the "Type" column: *cc* cover collapse sinkhole, *cs* cover suffusion sinkhole

Some authors have recently claimed that these sinkholes are due to collapse of the ceiling of natural caves in the Plio-Pleistocene calcarenite rock caused by the limited thickness of the cavities vault (from a few decimeters to a few meters at most), within an entirely carbonate setting (Delle Rose and Leucci 2010).

3.1 Sedimentology and stratigraphy

The rationale of this work requires a precise stratigraphic reconstruction for the correct identification of sinkhole typologies and for the interpretation of the results of the geophysical survey. It has been demonstrated that individual stratigraphic units show different susceptibility to formation of karst features; thus, detailed stratigraphical and sedimentological analyses and geologic mapping are essential in any study dealing with sinkhole identification, as well as for the selection of the most suitable management tools and remediation options (Hall 1976; Brezinski 2007; Zhou and Beck 2008).

Accordingly, the research involved a large set of data provided by our original field surveys and laboratory analyses, the collection of water-well and borehole data and the critical revision of more than 40 well-core stratigraphies supplied by local agencies and professionals. The available hydrological (piezometry, permeability), petro-physical and grain-size data from private consultants and the scientific literature (Cherubini et al. 1987; Andriani and Walsh 2002) have been normalized. The entire set of data has been organized in a geodatabase and visualized by GIS technologies.

Four litho-stratigraphical units have been distinguished. In descending stratigraphic order they are named (Fig. 3): Modern beach and dune deposits, Marsh deposits

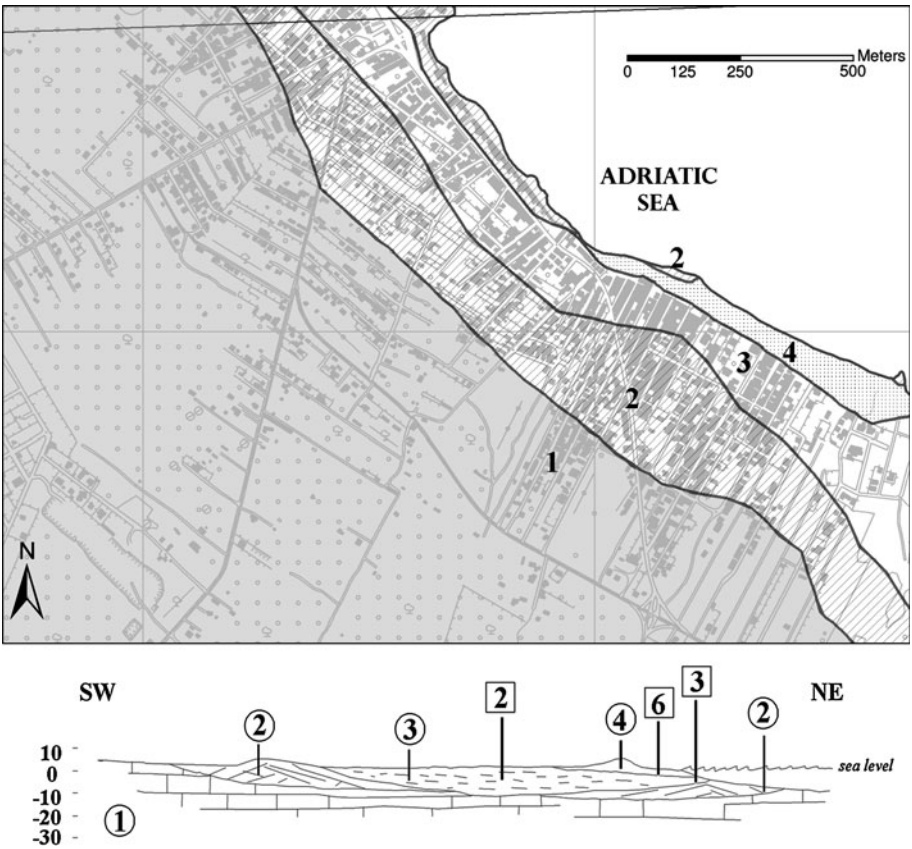

Fig. 3 Geological map and schematic section (vertical scale exaggerated) in the Casalabate area. *1* Gravina Calcarenite (Lower Pleistocene); *2* ancient dune deposits (Middle-Upper Pleistocene); *3* marsh deposits (Holocene); *4* modern beach and sand dune deposits. *Numbers in rectangles* indicate the sinkhole events reported in Table 1 and Fig. 2

(Holocene), Ancient eolian dune deposits (Middle-Upper Pleistocene) and Gravina Calcarenite (Lower Pleistocene).

3.1.1 Modern beach and dune deposits

The modern beach represents the foreshore and backshore areas of the present coastal zone. The foreshore deposits are formed by laminated sands gently sloping seawards, alternated with thin layers of shell fragments and laminae rich, or composed of dense minerals. The dune deposits are cross-stratified and may coalesce to form parabolic dunes. They form a ridge parallel to the present shoreline reaching a maximum elevation of 6 m.

A modern dune sample collected at Posto dei Trepuzzini was subjected to grain-size (sieving) and optical petrographic analysis (Folk 1974). The grain-size distribution, shown in Fig. 4, is very well sorted with a modal class in the fine-sand interval (0.250–0.125 mm) encompassing 85% of the distribution. The petrographic composition indicates that quartzose and (minor) feldspathic grains prevail on carbonate grains.

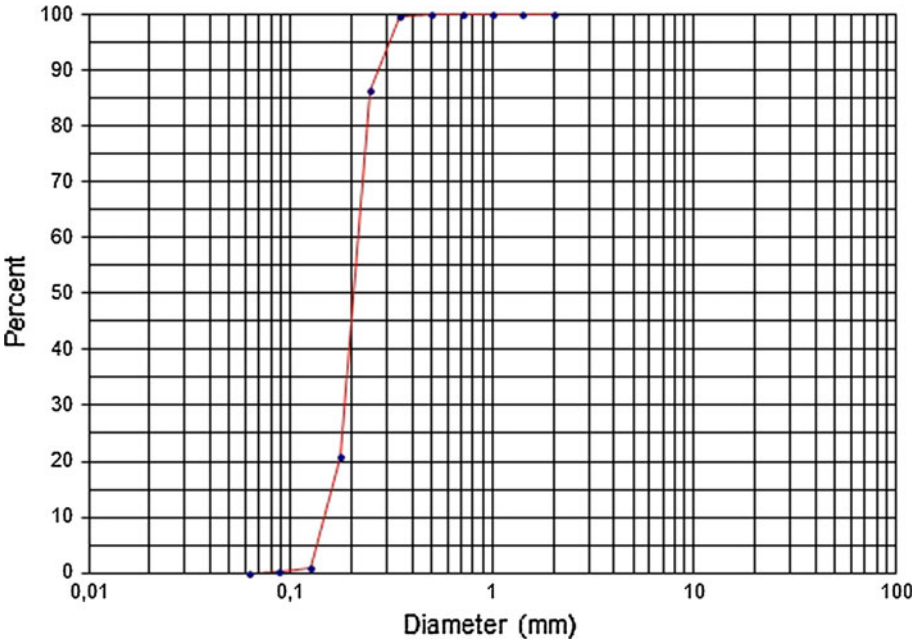

Fig. 4 Grain-size distribution of a modern sand dune sample collected at Casalabate

3.1.2 Marsh deposits (Holocene)

They consist of peat, with a considerable non-decomposed organic content and varying percentages of sandy mud and clay, reaching a maximum thickness of about 11 m. The organic content decreases with depth, while the clayey fraction and the plasticity index increases.

The degree of saturation of these deposits is always close to 100% and their characteristically low permeability protects the underlying shallow aquifer. The depositional environment is represented by coastal marsh depressions oriented parallel to the shoreline. These deposits overlie the Pleistocene eolian sediments; this contact is clearly visible in the foreshore zone when severe storm events remove the modern beach sand cover (Fig. 5).

3.1.3 Ancient eolian dune deposits (Middle-Upper Pleistocene)

They crop out both along the rocky segments of the Casalabate coast and landward. The succession is characterized by well-sorted cross-stratified calcarenites about 5 m thick. Macrofossils are totally absent. Landward these deposits create a morphological high, roughly parallel to the present coastline, well visible along some road cuts where they show a number of deformational features (Fig. 6). These deformation structures, concentrated in the lower part of the exposed section for a thickness of 1.7 m, are represented by irregular and narrow folds, regular antiforms and synforms and large vertical conduits bending the laminasets. In the upper part of the succession, about 1 m of undeformed eolian sands is present. These deformation features are identically detected in other nearby locations (Moretti 2000). The ancient eolian dune deposits include a backdune topsoil,

Fig. 5 Marsh sediments (*center*) and underlying ancient dune arenites (*right*) covered by modern sandy beach deposits outcropping along the present shoreline

generally composed of sand and silt, with low organic content, and overlie the Gravina Calcarenite hosting the upper part of the shallow aquifer.

Along the rocky coast, the ancient dune deposits are affected by a pervasive system of micro-faults and joints. Right-lateral strike-slip micro-faults strike N 090° with slips of about 0.5 m. Two main set of joints strike N 170° and N 145° in decreasing order of frequency. Both micro-faults and joints are filled with pebbly and sandy clasts.

A sample collected in the foreshore outcrop shown in Fig. 2 (Posto dei Trepuzzini) was used for grain-size (sieving) and petrography (thin-section optical microscopy) analyses. The resulting grain-size distribution indicates a modal class in the fine-sand size-interval and a very well-sorted size distribution. Interestingly, the grain-size distribution of the ancient and modern (Fig. 4) dune deposits is almost identical with their modal classes, respectively, encompassing 85 and 84% of the size distribution. From the petrographic analysis (Folk 1974), the proportions of Quartzose (Q), Feldspathic (F) and Lithic Grains (L) are: Q24, F8, L68. Q grains are dominated by unitary quartz crystals, F grains have a Plagioclase: K-feldspar ratio of 1:2 and the Lithics are almost exclusively carbonate grains.

Fig. 6 Eolian deposits showing deformation structures

Within carbonate grains the recalculated internal proportions are: 54% of micrite and biomicrite fragments, 25% of bio-lithoclasts and 21% of other carbonate rock fragments. The petrographic composition richer in quartz of the modern sand dunes above may be explained by the prolonged mechanical abrasion consuming increasing amounts of unstable carbonate grains in progressively younger deposits.

3.1.4 Gravina calcarenite (Lower Pleistocene)

This formation is the most ancient of the Salento Pleistocene succession and consists of coarse-grained yellowish calcarenites that unconformably overlie the carbonate units of Pliocene, Miocene and Cretaceous age and that crop out extensively landward. Its thickness varies considerably, reaching a maximum of more than 30 m. Mineralogically, the rock is composed of low-magnesium calcite with smaller amounts of kaolinite, illite, chlorite, smectite, gibbsite and goethite and scattered grains of quartz and feldspar (Andriani and Walsh 2002). The matrix is almost absent and the intragranular and intergranular porosity ranges from 42.9 to 49.4% so that the Gravina Calcarenite hosts most of the shallow aquifer.

3.2 Sinkhole history and morphology

Eight events in 18 years (time span 1993–2011) were registered at Casalabate (Table 1), all being concentrated at a short distance from the shoreline, plus an inland area nearby.

The most inland event occurred at a distance of some 126 m from the sea. One event (no. 3 in Table 1) occurred in the shoreface, about 30 m from the coastline.

It is not easy to provide a complete morphometric analysis of the sinkholes at Casalabate, since the events that interested the urban areas were not morphologically expressed as well-defined features, but rather as a generalized sinking of the ground, causing deformations and cracks in the buildings and man-made structures nearby. Nevertheless, the available data show that most of the sinkholes occur as circular to slightly elliptical features, spanning from 0.8 to 3 m in width, and from 0.4 to 3 m in depth (Table 1). The margins are generally vertical walls, where the calcarenite rock crops out in the lower part, and steeply inclined in the upper part, due to the sliding of the loose beach sand along the walls. If the sinkhole is not documented soon after its formation, it appears later as a funnel, with the bottom generally filled by sand.

The smallest features, as those that occurred in November 2010, may present more irregular shapes, locally triangular due to likely control exerted by discontinuities in the calcarenite below the sands. A high number of very small features (diameter 10 cm), partly aligned in the NW–SE direction, has also been observed along the beach.

The recognition of the sinkhole types of the area according to the classification by Waltham et al. (2005) results in the two following types, as indicated in the "Type" column in Table 1: cover collapse (cc) and cover suffusion (cs).

Cover collapse sinkholes occur due to presence of organic-rich clays above ancient eolian dune deposits and/or the carbonate bedrock (Gravina Calcarenites). Presence of karst caves within the soluble bedrock is at the origin of the process, which evolves through stoping of the cave vault, until reaching the contact with the layers above. At this stage, the consequent downward movement of materials from the surface layers, left unsupported, triggers the catastrophic and final phase of collapse.

Cover suffosion sinkholes, on the other hand, characterize the sites where incoherent deposits (Beach deposits) overlie the ancient eolian dune deposits through the interposition of thin (about 1 m) layers of organic-rich clays. The mechanisms of sinkhole formation in this case does not necessarily require the presence of a karst cave; simple conduits, or an increase in the overall porosity of the rock due to high percentage of micro-voids, are able to induce erosion of the loose material. In the Casalabate case, the erosion is also favored by the presence of a pervasive system of micro-faults and joints affecting the dune belt. The process may also be enhanced by groundwater flow and, being at a coastal site, by hyperkarst, with mixing of water of different nature (fresh vs. brackish). It is well known that such a mixing determines stronger aggressivity by water toward soluble rocks, thus increasing the development of karst processes (White 1990). Enlargement of the area affected by erosion may eventually lead to development of a sinkhole at the surface.

The two typologies of sinkholes above described show quite different morphologic features: cover collapse sinkholes present vertical walls, and a generally well-defined circular shape, with a diameter/depth ratio ranging from 3 to 1.5. On the contrary, cover suffosion sinkholes are characterized by a circular to elliptical shape, smaller depth and margins regularly sloping downward, according to the repose angle of loose materials; the result is a smoother morphology often masked by filling deposits.

The identification of the sinkhole type requires observation soon after its occurrence because the morphological features may be rapidly changed by later evolution and natural or man-made fill. At Casalabate, on the base of field observations and of the available documentation (pictures, technical reports, eyewitness and aerial photos), we were able to describe the eight cases listed in Table 1 as tentatively belonging to the cover collapse typology (5 events) and cover suffosion typology (3 events). In two out of eight cases

(no. 4 and 8 in Table 1) the available data were not sufficient to definitely assign the sinkhole to one or the other category.

In terms of natural hazard, cover collapse sinkholes are more dangerous due to the rapidity in the final phase of collapse. However, occurrence of cover suffosion sinkholes over wide areas, with coalescence of many sinkholes, may equally have serious effects on the built-up environment.

All that is presented above is in great contrast with the mechanism of collapse due to fall of the vault in caves within the bedrock invoked at Casalabate by Delle Rose and Leucci (2010); the geological data presented above, with particular regard to the stratigraphical succession, are in strong disagreement with such a model, which is based on a stratigraphy consisting exclusively of carbonate deposits, without taking into the due account the crucial presence of cover deposits above the calcarenite bedrock, and primarily that of the organic-rich clays.

3.3 Geophysics

Geophysical methods have been widely used for sinkhole studies, with particular reference to recognition of underground voids related to development of surface sinkholes (van Schoor 2002; Ardau et al. 2007; Jardani et al. 2007; Marcak et al. 2008; Ezersky et al. 2009; Kaufmann et al. 2011). Most of these papers focused on small areas encompassing one or few sinkholes, therefore with a great detail of analysis, and were essentially conducted for engineering aims. In the present paper, on the other hand, the purpose of the geophysical surveys is the possibility to identify and map, within a larger area, the sectors most susceptible to sinkholes. In this case it is important to identify the features related to likely sinkholes by contrasts in the physical properties (density, electrical resistivity, conductivity) with the surrounding sediments.

Different prospecting techniques are used to detect underground voids including seismic reflection and refraction (Grandjean and Leparoux 2004; Cardarelli et al. 2010), gravimetry (Butler 1984; Ardau et al. 2007), ground-penetrating radar (Dobecki and Upchurch 2006; Marcak et al. 2008) and electric resistivity tomography (Kim et al. 2007; Ezersky 2008). Success of each technique depends on its ability to reach the target depth with the appropriate resolution in different geological conditions.

Ground-penetrating radar (GPR) and electrical resistivity methods have been chosen for this study on the basis of the geological model (lithology and thickness of the units interested by sinkhole phenomena) and urbanization of the studied area.

The great advantage of GPR methods, compared with electrical resistivity, is that electrodes do not need to be inserted into the ground, thus allowing their use in urban areas. GPR is also characterized by rapid data acquisition, dense data coverage and high resolution.

To reach the objective we have carried out GPR surveys along many streets in the area (Fig. 7). The surveys were concentrated on the sectors where marsh deposits are present in the subsoil. To reduce the uncertainties in the interpretation of the results, the GPR profiles have been integrated with electrical resistivity tomography (ERT) investigations in selected areas.

The purpose of two-dimensional (2D) electrical resistivity profiling is to determine the subsurface electric resistivity distribution by taking measurements along a survey line at the surface. A measurement is normally performed by injecting electrical current into the ground through two current-carrying electrodes and measuring the resulting voltage difference at two potential electrodes. The apparent resistivity is calculated using the injected

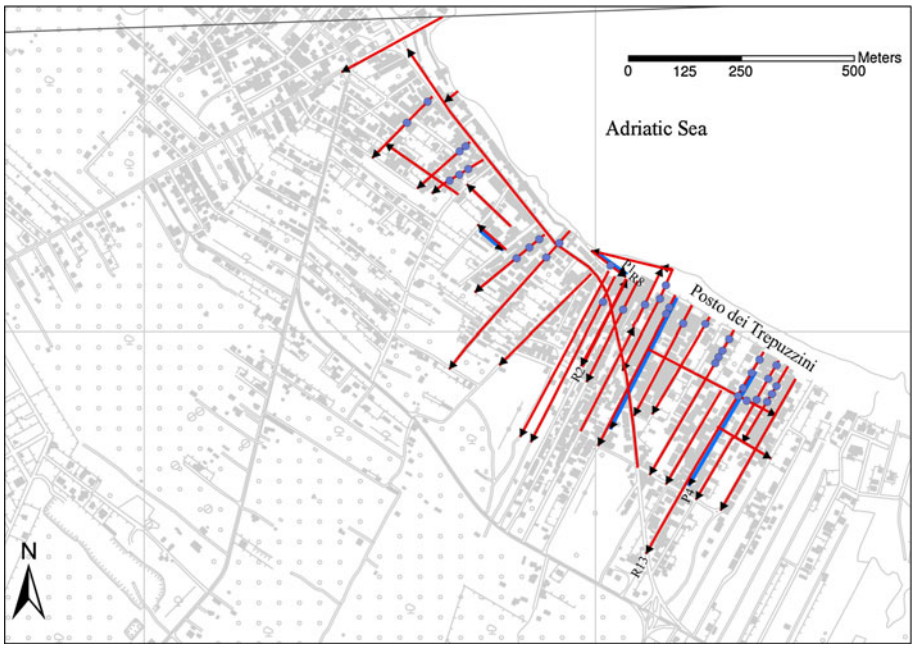

Fig. 7 Location of GPR and Geoelectrical profiles. *Blue circles* mark the GPR anomalies

current, the measured voltage and a geometric factor related to the arrangement of the four electrodes (Morelli and Labrecque 1996; Parasnis 1997).

Electrical resistivity methods reach greater depths than GPR, but with lower resolution. At Casalabate, given the geological setting, and in particular the strong dispersion of the GPR signal in the marsh deposits (which was the main drawback below the first meters of investigation), ERT was considered to be the best method to support the extensive aerial coverage of GPR, and to have further information at greater depth.

3.3.1 GPR and ERT data acquisition and interpretation

A SIR 3000 of the GSSI system with central antenna frequency of 400 MHz was used for GPR surveys. In total 27 GPR profiles were realized, for more than 10,000 m of linear survey (Fig. 7). Some test profiles have been carried out using 50, 60, 100 ns time windows, to appraise the depth of investigation of the electromagnetic waves and to choose the time window and therefore the depth of best investigation. The best results have been obtained with the 100 ns time window. The acquired parameters (time window, gain function, filters) were kept constant for all the profiles to facilitate data comparison. To convert time scale in depth scale, the wave propagation velocity in the ground between hyperbolae fitting using the diffraction hyperbola method (Reynolds 1997) with a mean value of 9 cm/ns has been considered.

The GPR data processing includes sequential zero-time corrections, trace editing and normalization of the horizontal scale sampling intervals of 0.025 m, and 2D filter background removal. Choice of the spar frequency was dictated by size of the target (from decimetric to metric in both lateral and vertical direction) so that the most proper spar for this purpose was considered to be the 400 MHz. The penetration differences and shape of the

reflection observed in the radar section represent the variations in the underground electromagnetic behavior that define stratigraphical changes and correlated anomalies (Fig. 6).

ERT measurements are carried out along a survey line with various combinations of electrodes and spacing to produce an apparent resistivity cross-section (Reynolds 1997). Apparent resistivity data are then inverted to generate a model of the subsurface structure and stratigraphy based on its electrical properties. Resistivity data were inverted with L2 norm-based least-squares optimization method, the smoothness-constrained by De Groot-Hedlin and Constable (1990), used the RES2DINV, distributed by Geotomo Software.

ERT was performed along six lines (Fig. 7) using a IRIS-Syscal Plus. We used two different array configurations (dipole–dipole and Wenner) and a multi-electrode system with 48 and 24 electrodes, respectively, 1-, 2- and 3 m-spaced. The investigation depth increases with the increasing distance between electrodes. The maximum investigation depth for this array range from 4 to 19 m.

These profiles, labeled P1 to P5, overlap the R8, R13, R16, R27 GPR profiles (Fig. 7).

Figure 7a shows a radar section relative to a profile running sub-parallel to the coastline near the sea. The section shows clearly areas with higher signal penetration and undulated reflections labeled "A," areas where the signal radar is attenuated labeled "B," with only occasionally hyperbolic reflections labeled "C." Based upon the previously presented geological data, these data may be interpreted as marking the contact between marsh deposits (B) overlying eolian deposits (A). Presence of the anomalies (C) is not explainable with the typical stratigraphy of the area, and these could be therefore related to premonitory signs of active sinkhole phenomena (for instance voids due to collapse of marsh deposits). A fortunate circumstance allowed to directly observe the collapse just in correspondence of the anomaly detected by the R8 profile (Fig. 8b).

The interpreted radar section has been integrated with an ERT profile. The main purpose of the ERT surveys was to identify by contrasts in the electrical resistivity, the surface between marsh deposits and the underlying eolian deposits, as well as to clarify the anomalies (C) previously interpreted as indicators of active sinkhole phenomena.

The final inversion results of the ERT sections have been analyzed and interpreted in combination with the boreholes and GPR data. The following electrical stratigraphy can be described from examination of the resistivity model shown in Fig. 8c: the beach sand deposits have a maximum thickness of 0.5 m and are characterized by resistivity values of 4–5 ohm m; below the beach deposits, a 1-m-thick layer labeled "B" (visible in the 0–28 m X-axis) is characterized by 0.5–2 ohm m resistivity values. These values are typical of clay sediments such as marsh deposits. This electro-layer overlies another layer (A) with resistivity values >5 ohm m, associated to the eolian deposits. The latter shows heterogeneous values which probably reflect the inhomogeneous permeability characters of the deposits: where they are fractured the resistivity value decreases to 3 ohm m due to high saturation degree, whereas, on the contrary, when they are compact the resistivity values increase to 50 ohm m.

The P1 profile intercepts the sinkhole individuated with R8 GPR profile, at 28 m along axis X. At the moment of the ERT survey, this sinkhole was filled. The profile shows clearly the high potentiality of ERT to determine the geometry and evolution of collapse sinkhole. The B layer (Fig. 8c) shows, in correspondence of the sinkhole, an irregular top and the base that abruptly moves downwards about 1 m.

Figure 9 shows the R13 GPR and P4 ERT profiles (see Fig. 7 for location), carried out perpendicularly to the coastline, in a urban setting. Both profiles confirm the interpretation of the geological surveys. The contact between marsh and eolian deposits is always well visible and marked by an attenuation of the radar signal in the sand-clay sediments and by

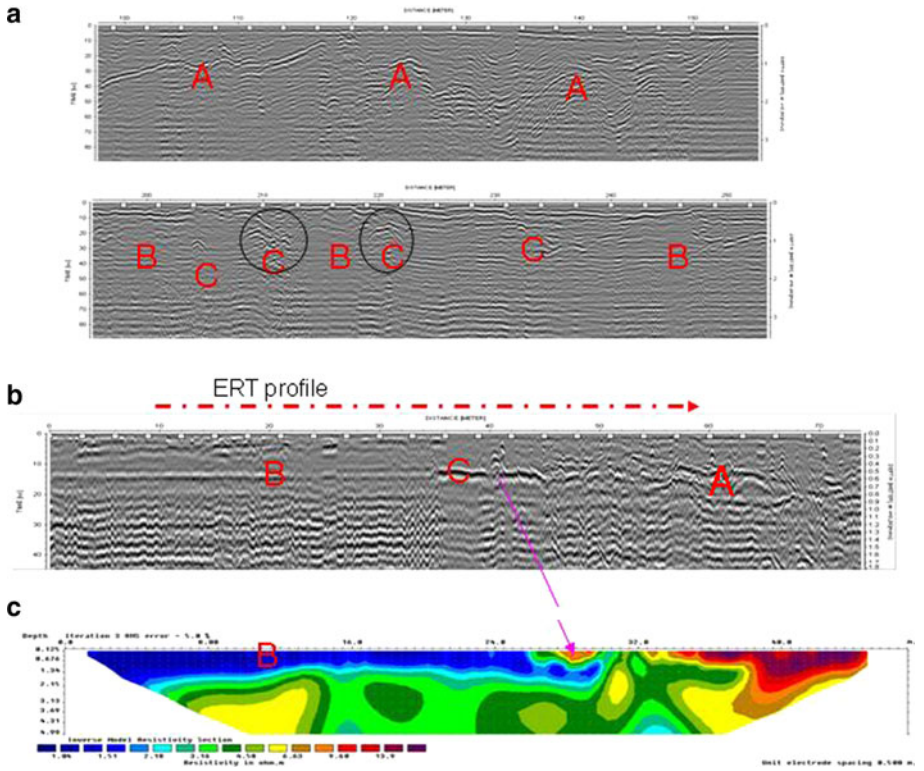

Fig. 8 Example of geophysical analysis (see Fig. 7 for location): **a** R2 profile: 400 MHz radar reflection profile; *A* eolian dune deposits, *B* marsh deposits, *C* active sinkhole phenomena, **b** R8 profile: 400 MHz radar reflection profile, **c** resistivity model related to P1 profile

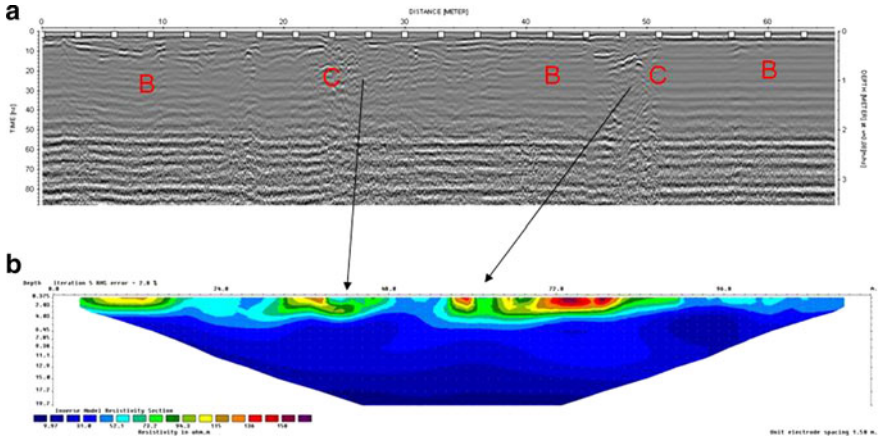

Fig. 9 Example of geophysical analysis (see Fig. 7 for location): **a** R13 profile: 400 MHz radar reflection; *B* marsh deposits, *C* active sinkhole phenomena, **b** resistivity model related to P4 profile

a low increase of the resistivity values at the passage to the calcarenites. The sinkholes are marked by radar hyperbolic reflections and their geometry is well recognizable by ERT.

The conducted surveys highlight the potentiality of GPR to identify active sinkholes and to determine the lithostratigraphic contacts. ERT proves to be an optimal indicator of the geometry of the sinkholes, providing interesting information about their evolution.

4 Sinkhole susceptibility assessment

The results of the detailed geologic mapping provide a good basis for assessing potential damage to infrastructures and people, because the distribution of sinkholes is controlled primarily by the geology of the bedrock. The map of the litho-stratigraphic units and the sinkhole distribution demonstrate the correlation between the spatial occurrence of the events and the rock types (Fig. 10). Sinkholes are very frequent and have caused catastrophic damage to buildings where the marsh deposits reach their maximum thickness; at the same time, they are also common where these deposits are thin and buried by sandy beach sediments. In this case, sinkholes occur generally as cover suffosion typology and are of minor size. This distinction, once again, highlights the crucial importance of recognizing the geological model for correctly defining the sinkhole typologies acting in the area.

Fig. 10 Sinkhole susceptibility map at Casalabate. *Red color* indicates the high susceptibility areas (HS); *pale blue* the susceptible areas (IS); *green* the medium to low susceptible areas (LS); *white* the not susceptible areas (NS)

Interpretation of the ground penetration radar and electrical tomography profiles allowed to add further information by identifying the potentially most unstable areas, significantly improving the assessment of the sinkhole-prone areas (Fig. 10).

GPR signal was strongly absorbed in those sectors with presence of organic materials, but, at the same time, it highlighted several anomalies, likely related to sinkholes. The ancient eolian dune belt was, on the other hand, well indicated by a good propagation of the electromagnetic waves, while the geoelectric tomography resulted in a 2D-visualization of the subsoil by means of resistivity distribution models. The latter technique, in particular, beside confirming the thickness of palustrian deposits, was also able to identify the presence of voids in the areas, likely indicators of sinkholes.

Several methodologies have been proposed to assess the susceptibility to the development of sinkholes. These are principally based on numerical models and expert judgement (Edmonds et al. 1987; Gutierrez 1998; Kourgialas and Karatzas 2011; Tharp 1999, 2002; Kaufmann 2008), and on spatial distribution of the events mapped with morphological and/or geophysical methodologies (Gutierrez-Santolalla et al. 2005; Bruno et al. 2008; Galve et al. 2008; Garcia-Moreno and Mateos 2011). In most of the cases, the approaches presented in the scientific literature consist of modeling of individual sinkholes (Tharp 1999, 2002; Parise and Lollino 2011) or in production of susceptibility maps implemented in GIS environment at the regional or local scale (Edmonds et al. 1987; Gutierrez-Santolalla et al. 2005; Bruno et al. 2008; Kaufmann 2008). The study by Galve et al. (2008), on the other hand, is probably the most complete so far, making an attempt in performing a statistical analysis between the mapped sinkholes and a set of conditioning factors, and validating the obtained models by means of a random-split strategy (Galve et al. 2008). In any case, different approaches to assess the sinkhole susceptibility are present in the literature, and it appears that choice of the most proper approach should be essentially dictated by the sinkhole population, with particular regard to size of the examined features (in terms of diameter and depth), and the overall extension of the study area as well (Tolmachev and Leonenko 2011). High complexity of the models and/or of the statistical analysis performed do not necessarily correspond to better results in terms of prediction of the phenomena.

Given the limited areal coverage of the site, and the before described very peculiar features of the observed sinkholes, in this paper, with the purpose of producing a susceptibility map at Casalabate, the following criteria were adopted:

1. proximity to already occurred sinkholes: the areas located within a buffer of 10 m from the registered events are mapped as highly susceptible (HS);
2. geological conditions favoring sinkhole formation (presence of marsh deposits) and presence of a high density of GPR anomalies: these areas are classified as having intermediate susceptibility (IS);
3. geological conditions favoring sinkhole formation (presence of marsh deposits) without GPR anomalies: these areas are classified as belonging to medium to low susceptibility class (LS);
4. absence of geological conditions favoring sinkhole formation and absence of GPR anomalies: these areas are mapped as not susceptible (NS).

The results of the application of this methodology are shown in Fig. 10. The HS areas occupy 3.791 mq (that is 0.2% of Casalabate) and correspond with the sectors where the marsh deposits reach the maximum thickness. The IS (37.392 mq, that is 1.8%) and LS (766.504 mq, that is 36.9% of Casalabate) classes occupy a large stretch parallel to the coastline; it has to be remarked that these areas host the maximum density of tourists

during the summer season. The NS areas correspond to those in which fossil dune belt and Gravina Calcarenites crop out; they are characterized in the Casalabate area by scarce density of human occupation.

5 Conclusions

An integrated approach involving stratigraphy, geomorphology and geophysics is here used to develop a methodology aimed at studying built-up coastal areas where the occurrence of sinkholes has been ascertained, and at obtaining a zonation of the related susceptibility. This topic is of great interest in the Apulia region of southern Italy, where long stretches of coastline have been interested in recent decades by heavy, often not controlled, urban expansion. The proposed methodology has been applied at Casalabate, a small village along the Adriatic coast where since 1990 several cases of sinkholes have been registered.

Detailed stratigraphic analysis has been carried out by means of direct and indirect surveys, integrated by critical review of the data available in the literature. Geologic maps are the principal tools for displaying and conveying data important in the identification of factors for sinkhole distribution. The results of these stratigraphic studies are significantly in contrast with the model at this same site previously presented in literature (Delle Rose and Leucci 2010): rather than considering a whole carbonate setting, our reconstruction highlights a tentative correlation between distribution of the sinkholes and those areas interested by the presence of marsh deposits overlying a carbonate karstified bedrock, a geological condition which is common in many urbanized coastal areas of Salento. The detail provided in the reconstruction of the local stratigraphy at Casalabate was crucial for the correct identification of the sinkhole typologies that, in turn, is a mandatory step in order to properly focus the successive studies and the mitigation projects in sinkhole-prone areas.

Geophysical surveys proved to be useful to better define the geological model at Casalabate. Integration of different geophysical techniques, in particular, demonstrated the need to crosscheck the results deriving from each single method, in order to collect the greatest amount of possible information.

As final outcome of the study, a susceptibility zonation map has been produced. Although phenomena such as sinkholes cannot be precisely forecasted, this map is particularly useful to identify the areas most prone to sinkhole (De Waele et al. 2011b). Coupled with additional information deriving from chronology of the events so far occurred, the susceptibility map may represent an important tool to be considered for planning and development purposes. In addition, since long stretches of the Apulian coastline are affected by sinkhole events, such an approach may represent a significant tool to face the risk posed by sinkhole in similar low-lying coasts, heavily interested by urbanization.

In terms of hazard, the small number of available documented data do not allow any temporal analysis which could forecast the possibility of sinkhole occurrence in the next future. However, based upon the recorded events, a frequency of occurrence of about one sinkhole every 2 years is documented, which points out to the need to thorough monitoring activities and studies in the area.

References

Andriani G, Walsh N (2002) Physical properties and textural parameters of calcarenitic rocks: qualitative and quantitative evaluations. Eng Geol 67:5–15

Ardau F, Balia R, Bianco M, De Waele J (2007) Assessment of cover-collapse sinkholes in SW Sardinia (Italy). In: Parise M, Gunn J (eds) Natural and anthropogenic hazards in karst areas: recognition, analysis and mitigation. Geological Society, London, pp 47–57 Special publication 279

Boenzi F, Caldara M, Pennetta L, Simone O (2006) Environmental aspects related to the physical evolution of some wetlands along the Adriatic coast of Apulia (Southern Italy): a review. J Coast Res 39:170–175

Bosellini A, Bosellini FR, Colalongo ML, Parente M, Russo A, Vescogni A (1999) Stratigraphic architecture of the Salento coast from Capo d'Otranto to S. Maria di Leuca (Apulia, southern Italy). Riv Ital Paleontol Stratigr 105:397–415

Bossio A, Foresi ML, Margiotta S, Mazzei R, Salvatorini G, Donia F (2006) Stratigrafia neogenico-quaternaria del settore nord-orientale della Provincia di Lecce (con rilevamento geologico alla scala 1:25.000). Geologica Romana 39:63–88

Brezinski KD (2007) Geologic and anthropogenic factors influencing karst development in the Frederick region of Maryland. Environ Geosci 14(1):31–48

Bruno E, Calcaterra D, Parise M (2008) Development and morphometry of sinkholes in coastal plains of Apulia, southern Italy. Preliminary sinkhole susceptibility assessment. Eng Geol 99:198–209

Butler DK (1984) Microgravimetric and gravity gradient techniques for the detection of subsurface cavities. Geophysics 49:1084–1096

Cardarelli E, Cercato M, Cerreto A, Di Filippo G (2010) Electrical resistivity and seismic refraction tomography to detect buried cavities. Geophys Prospect 58:685–695

Cherubini C, Margiotta B, Sgura A, Walsh N (1987) Caratteri geologico-tecnici dei terreni della città di Brindisi. Mem Soc Geol Ital 37:689–700

Cotecchia V, Dai Pra G, Magri G (1969) Oscillazioni tirreniane e oloceniche del livello del mare nel Golfo di Taranto, corredate da datazioni con il metodo del radiocarbonio. Geol Appl Idrogeol 4:93–148

Cotecchia V, Dai Pra G, Magri G (1971) Sul Tirreniano della costa ionica salentina (Puglia). Datazione su campione di coralli con il metodo 230Th/234U. Geol Appl Idrogeol 6:105–112

De Groot-Hedlin C, Constable S (1990) Occam's inversion to generate smooth, two-dimensional models from magnetotelluric data. Geophysics 55:1613–1624

De Waele J, Lauritzen SE, Parise M (2011a) On the formation of dissolution pipes in Quaternary coastal calcareous arenites in Mediterranean settings. Earth Surf Process Land 36:143–157

De Waele J, Gutierrez F, Parise M, Plan L (2011b) Geomorphology and natural hazards in karst areas: a review. Geomorphology 134:1–8

Del Prete S, Iovine G, Parise M, Santo A (2010) Origin and distribution of different types of sinkholes in the plain areas of Southern Italy. Geodinamica Acta 23(1/3):113–127

Delle Rose M, Leucci G (2010) Towards an integrated approach for characterization of sinkhole hazards in urban environments: the unstable coastal site of Casalabate, Lecce, Italy. J Geophys Eng 7:143–154

Delle Rose M, Parise M (2002) Karst subsidence in south-central Apulia. Italy Int J Speleol 31(1/4):181–199

Delle Rose M, Parise M (2004) Slope instability along the Adriatic coast of Salento, southern Italy. In: Proceedings of IX international symposium on landslides, Rio de Janeiro (Brasil), 28 June–2 July 2004, vol 1, pp 399–404

Delle Rose M, Parise M (2005) Speleogenesi e geomorfologia del sistema carsico delle Grotte della Poesia nell'ambito dell'evoluzione quaternaria della costa Adriatica Salentina. Atti e Memorie Commissione Grotte "E. Boegan" 40:153–173

Delle Rose M, Federico A, Parise M (2004) Sinkhole genesis and evolution in Apulia, and their interrelations with the anthropogenic environment. Nat Hazards Earth Syst Sci 4:747–755

Denitto F, Moscatello S, Palmisano P, Poto M, Onorato R (2006) Novità speleologiche, idrologiche e naturalistiche della Palude del Capitano (pSIC IT9150013), Costa Neretina (Lecce). Thalassia Salentina 29:99–116

Dobecki TL, Upchurch SB (2006) Geophysical applications to detect sinkholes and ground subsidence. Lead Edge 25:336–341

Edmonds C, Green C, Higginbottom I (1987) Subsidence hazard prediction for limestone terrains as applied to the English Cretaceous chalk. Geol Soc Eng, Special Publication 4, pp 283–293

Ezersky M (2008) Geoelectric structure of the Ein Gedi sinkhole occurrence site at the Dead Sea shore in Israel. J Appl Geophys 64:56–69

Ezersky M, Legchenko A, Camerlynck C, Al-Zoubi A (2009) Identification of sinkhole development mechanism based on a combined geophysical study in Nahal Hever South area (Dead Sea coast of Israel). Environ Geol 58:1123–1141

Folk RL (1974) Petrology of sedimentary rocks. Hemphill's, Austin, TX

Forth RA, Butcher D, Senior R (1999) Hazard mapping of karst along the coast of the Algarve, Portugal. Eng Geol 52(1–2):67–74

Galve JP, Bonachea J, Remondo J, Gutierrez F, Guerrero J, Lucha P, Cendrero A, Gutierrez M, Sanchez JA (2008) Development and validation of sinkhole susceptibility models in mantled karst settings. A case study from the Ebro valley evaporite karst (NE Spain). Eng Geol 99:185–197

Garcia-Moreno I, Mateos RM (2011) Sinkholes related to discontinuous pumping: susceptibility mapping based on geophysical studies. The case of Crestatx (Majorca, Spain). Environ Earth Sci 64:523–537

Grandjean G, Leparoux D (2004) The potential of seismic methods for detecting cavities and buried objects: experimentation at a test site. J Appl Geophys 56:93–106

Gutierrez F (1998) Subsidencia por colapso en un karst alluvial. Analisis de estabilidad. In: Gomez-Ortiz A, Salvador Franch F (eds) Investigaciones recientes de la geomorfologia espanola. V Reunion Nacional de Geomorfologia, Barcelona, pp 47–58

Gutierrez-Santolalla F, Gutierrez Elorza M, Marin C, Desir G, Maldonado C (2005) Spatial distribution, morphometry and activity of La Puebla de Alfiden sinkhole field in the Ebro River Valley (NE Spain): applied aspects for hazard zonation. Environ Geol 48:360–369

Hall DR (1976) Stratigraphy and origin of surficial deposits in sinkholes in south-central Indiana. Geology 4(8):507–509

Harding JL (1999) Environmental change during the Holocene in south east Italy: an integrated geomorphological and palynological investigation. Larix Books, Sheffield, p 148

Hearty PJ, Dai Pra G (1992) The age and stratigraphy of Middle Pleistocene and younger deposits along the Gulf of Taranto (Southeast Italy). J Coastal Res 8:82–105

Jardani A, Revil A, Santos F, Fauchard C, Dupont JP (2007) Detection of referential infiltration pathways in sinkholes using joint inversion of self-potential and EM-34 conductivity data. Geophys Prospect 55:749–760

Kaufmann JE (2008) A statistical approach to karst collapse hazard analysis in Missouri. In: Yyuhr LB, Calvin Alexander E, Beck BF (eds) Sinkholes and the engineering and environmental impacts of karst, 183. ASCE Geotechnical Special Publication, Huntsville, pp 257–268

Kaufmann G, Romanov D, Nielbock R (2011) Cave detection using multiple geophysical methods: Unicorn cave, Harz Mountains, Germany. Geophysics 76(3):B71–B77

Kim JH, Yi MJ, Hwang SH, Song Y, Cho SJ, Synn JH (2007) Integrated geophysical surveys for the safety evaluation of a ground subsidence zone in a small city. J Geophys Eng 4:332–347

Kourgialas NN, Karatzas GP (2011) Flood management and a GIS modelling method to assess flood—hazard areas—a case study. Hydrol Sci J 56(2):212–225

Marcak H, Golebiowski T, Tomecka-Suchon S (2008) Geotechnical analysis and 4D GPR measurements for the assessment of the risk of sinkholes occurring in a Polish mining area. Near Surf Geophys 6(4):233–243

Margiotta B (1997) Dinamica degli spazi costieri: le Cesine (Lecce). Lecce, Oistros, p 61

Margiotta S, Negri S (2005) Geophysical and stratigraphical research into deep groundwater and intruding seawater in the Mediterranean area (the Salento Peninsula, Italy). Nat Hazards Earth Syst Sci 5:127–136

Margiotta S, Mazzone F, Negri S (2010) Stratigraphic revision of Brindisi-Taranto Plain: hydrogeological implications. Memorie Descrittive della Carta Geologica d'Italia 90:165–180

Mastronuzzi G, Sansò P (2002) Holocene coastal dune development and environmental changes in Apulia (southern Italy). Sediment Geol 150:139–152

Morelli G, Labrecque DJ (1996) Advances in ert inverse modelling. Eur J Environ Eng Geophys 1:171–186

Moretti M (2000) Soft-sediment deformation structures interpreted as seismites in middle-late Pleistocene eolian deposits (Apulian foreland, southern Italy). Sediment Geol 135:167–179

Moretti M, Owen G, Tropeano M (2011) Soft-sediment deformation induced by sinkhole activity in shallow marine environments: a fossil example in the Apulian Foreland (Southern Italy). Sediment Geol 235:331–342

Norris RM, Back W (1990) Erosion of seacliff by groundwater. In: Higgins CG, Coates DR (eds) Groundwater geomorphology: the role of subsurface water in earth-surface processes and landforms. Geological Society of America Special Paper 252, pp 283–290

Palmentola G (1987) Lineamenti geologici e morfologici del Salento leccese. Quad Ric Centro Studi Geotec e d'Ing 11:7–23

Parasnis DS (1997) Principles of applied geophysics, 5th edn. Chapman & Hall, London

Parise M (2008) I sinkholes in Puglia. In: Nisio S. (ed) I fenomeni naturali di sinkhole nelle aree di pianura italiane. Memorie Descrittive della Carta Geologica d'Italia 85:309–334

Parise M, Lollino P (2011) A preliminary analysis of failure mechanisms in karst and man-made underground caves in Southern Italy. Geomorphology 134(1–2):132–143

Primavera M, Simone O, Fiorentino G, Caldara M (2011) The paleoenvironmental study of the Alimini Piccolo Lake enables a reconstruction of Holocene sea level changes in southeast Italy. Holocene 21:553–563

Reynolds JM (1997) An introduction to applied and environmental geophysics. Wiley, New York

Tharp TM (1999) Mechanics of upward propagation of cover collapse sinkhole. Eng Geol 52:23–33

Tharp TM (2002) Poroelastic analysis of cover-collapse sinkhole formation by piezometric surface drawdown. Environ Geol 42:447–456

Tolmachev V, Leonenko M (2011) Experience in collapse risk assessment of building on covered karst landscapes in Russia. In: van Beynen P (ed) Karst management. Springer, Berlin, pp 75–102

van Schoor M (2002) Detection of sinkholes using 2D electrical resistivity imaging. J Appl Geophys 50:393–399

Waltham T, Bell FG, Culshaw MG (2005) Sinkholes and subsidence: karst and cavernous rocks in engineering and construction. Springer, Praxis, p 382

White WB (1990) Surface and near-surface karst landforms. In: Higgins CG, Coates DR (eds) Groundwater geomorphology: the role of subsurface water in earth-surface processes and landforms. Geological Society of America Special Paper 252, pp 157–175

Zhou W, Beck BF (2008) Management and mitigation of sinkholes on karst lands: an overview of practical applications. Env Geol 55:837–851